Organic & Biomolecular Chemistry

Cite this: *Org. Biomol. Chem.*, 2012, **10**, 6951

www.rsc.org/obc

PAPER

Anion binding in aqueous media by a tetra-triazolium macrocycle†

Nicholas G. White,[a] Sílvia Carvalho,[b] Vítor Félix[b] and Paul D. Beer*[a]

Received 15th May 2012, Accepted 27th June 2012
DOI: 10.1039/c2ob25934f

Three tetra-triazole macrocycles were synthesized in good yields by the copper(I)-catalysed cycloaddition of bis-triazole azides and bis-alkynes. One of these was alkylated to give a cyclic tetra-triazolium receptor, which complexes anions strongly in competitive DMSO–water mixtures. In 1 : 1 DMSO–water, the tetracationic receptor exhibits a preference for the larger halides, bromide and iodide, with all halides associating more strongly than the oxoanion, acetate. The sulfate dianion is complexed far more strongly than any of the monobasic anions ($K_a > 10^4$ M^{-1}). Quantum mechanics/molecular mechanics simulations corroborate the experimentally determined anion binding selectivity trends.

Introduction

Since initial reports of the regioselective synthesis of the 1,2,3-triazole motif by copper(I)-catalysed cycloaddition of azides and alkynes (CuAAC),[1,2] this heterocycle has found widespread use across many areas of chemistry. In 2008, Flood,[3,4] Craig,[5] and Hecht[6] demonstrated that oligomeric or macrocyclic poly-triazole systems are capable of interacting with halide anions through C–H···anion interactions alone in organic solvents, and in subsequent years the triazole functionality has been incorporated into a variety of acyclic[7–13] and macrocyclic anion receptors.[3,4,14–21]

With a few notable exceptions,[22–28] the design of anion receptors that function in competitive aqueous media has relied on the integration of positive charge into the host structural framework.[29–32] For example, several years ago we reported alkyl-linked tetra-imidazolium and -benzimidazolium macrocycles which exhibit selectivity for fluoride over the other halides in 9 : 1 CD_3CN–D_2O solvent mixtures (Fig. 1).[33]

In spite of the current interest in triazole-based systems, the exploitation of the *triazolium* motif for anion recognition applications has remained largely unexplored.[34–40] This is surprising given that the additional positive charge, resulting from alkylation, further polarises the heterocycle's C–H bond, as well as increasing electrostatic interactions with the anion. Herein we describe the synthesis of a tetra-triazolium macrocycle, which binds anionic guest species in competitive aqueous solvent mixtures through charge-assisted C–H···anion hydrogen bonding.

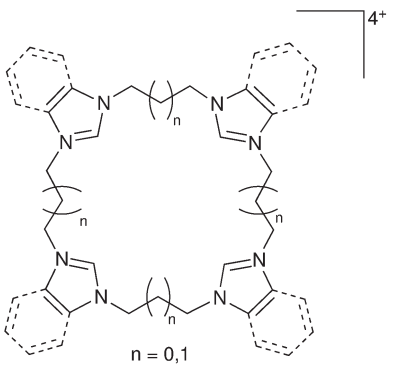

Fig. 1 Previously reported tetra-imidazolium and -benzimidazolium macrocyclic anion hosts that bind fluoride selectively in 9 : 1 CD_3CN–D_2O.[33]

Results and discussion

Receptor synthesis

We reasoned that rigid tetra-triazole aryl macrocycles, such as those reported by Flood,[3,4,15] would be a challenge to fully alkylate, both in terms of the difficulty of completely alkylating a highly conjugated system, and of the possibility of yielding highly insoluble products. Therefore we targeted the less rigid macrocycles, **1**, **2** and **3** (Scheme 1), in the hope that anion binding affinity lost by the diminished degree of preorganisation would be compensated by the increased binding strength resulting from greater electrostatic interactions.

The receptors were synthesized using a general strategy, which allows access to a wide range of symmetric or non-symmetric

[a]*Chemistry Research Laboratory, Department of Chemistry, University of Oxford, South Parks Road, Oxford, OX1 3TA, United Kingdom. E-mail: paul.beer@chem.ox.ac.uk; Fax: +44 (0)1865 272690; Tel: +44 (0)1865 285142*
[b]*Departamento de Química, CICECO and Secção Autónoma de Ciências da Saúde, Universidade de Aveiro, 3810-193 Aveiro, Portugal*

† Electronic supplementary information (ESI) available: NMR spectra of new compounds, titration protocols, details of modelling. CCDC 881646–881649. For ESI and crystallographic data in CIF or other electronic format see DOI: 10.1039/c2ob25934f

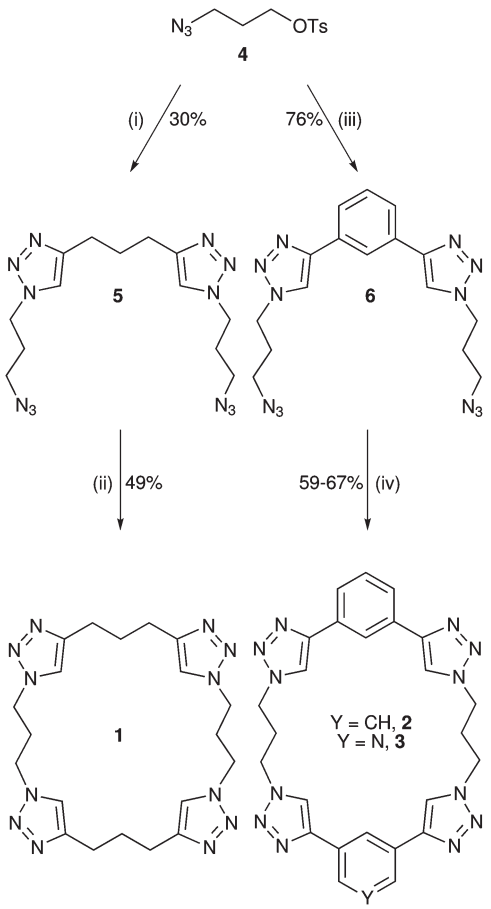

Scheme 1 Synthesis of tetra-triazole macrocycles, **1**, **2** and **3**. Conditions and reagents: (ia) 1,6-heptadiyne, $[Cu^{I}(CH_3CN)_4](PF_6)$, TBTA, DIPEA, CH_2Cl_2, (ib) NaN_3, DMSO, 60 °C, 30% from 1,6-heptadiyne; (ii) 1,6-heptadiyne, $[Cu^{I}(CH_3CN)_4](PF_6)$, TBTA, DIPEA, CH_2Cl_2, 49%; (iiia) 1,3-diethynylbenzene, $[Cu^{I}(CH_3CN)_4](PF_6)$, TBTA, DIPEA, CH_2Cl_2, (iiib) NaN_3, DMSO, 76% from 1,3-diethynylbenzene; (iv) 1,3-diethynylbenzene or 3,5-diethynylpyridine, $[Cu^{I}(CH_3CN)_4](PF_6)$, TBTA, DIPEA, CH_2Cl_2, 67% for **2**, 59% for **3**.

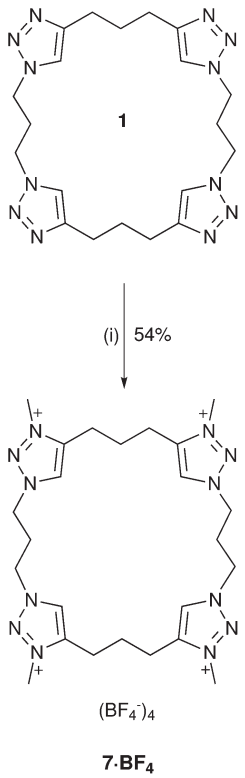

Scheme 2 Synthesis of **7**·$\mathbf{BF_4}$. Conditions and reagents: (i) $(Me_3O)(BF_4)$, CH_2Cl_2, 54%.

tetra-triazole macrocycles. The commercially available bis-alkynes, 1,6-heptadiyne and 1,3-diethynylbenzene were reacted with 3-azidopropoxytosylate, **4**,[41] under CuAAC conditions to give the bis-triazole tosylates. Reacting these with sodium azide in DMSO gave the bis-triazolyl azides, **5** and **6**. The CuAAC cyclisation reaction of these bis-azides and one equivalent of a bis-alkyne under pseudo high dilution conditions (1.0 mmol L^{-1} in dichloromethane) gave the desired macrocycles, **1**, **2** and **3** in good yields (49–67%) after purification by column chromatography (Scheme 1).

Attempts to alkylate **2** and **3** were hampered by their low solubility in common solvents, which ruled out the use of $(Me_3O)(BF_4)$. Partial alkylation of **2** was possible using benzyl bromide in the microwave at 120 °C, giving a mixture of mono- and di-cationic species along with unreacted starting material, as evidenced by TLC and ESI-MS. Attempts to alkylate further using higher temperatures caused decomposition of the triazole groups. It was possible to selectively alkylate **3** at the pyridine group using methyl iodide or bromohexadecane, but initial investigations showed that these alkylated compounds were poorly soluble, hampering chromatographic purification procedures.

Pleasingly, **1** has good solubility in a range of organic solvents. A solution of **1** in dry dichloromethane containing five equivalents (*i.e.* 1.25 equivalents per triazole group) of $(Me_3O)(BF_4)$ was stirred for two days at room temperature. The resulting crude solid was recrystallised from ethanol–acetonitrile (6 : 1) to give the tetra-cationic product, **7**·$\mathbf{BF_4}$, as white crystals in 54% yield (Scheme 2).

X-ray crystallography

Crystals of **2** suitable for single crystal X-ray structural analysis were obtained from two different solvent systems. Slow vapour diffusion of dichloromethane into a d_6-DMSO solution of the macrocycle gave solventless crystals, while the slow evaporation of a very dilute solution of **2** in 3 : 1 methanol–water gave crystals of the trihydrate **2**·$3(H_2O)$. The two structures are shown in Fig. 2. Interestingly, in the solventless crystal, the macrocycle has a very open structure, while **2**·$3(H_2O)$ exhibits a folded structure, presumably due to solvophobic effects. The single crystal structures of the propyl-linked macrocycles, **1** and **7**·$\mathbf{BF_4}$ were also obtained—the neutral macrocycle crystallizes without solvent, the tetracationic receptor as the acetonitrile adduct (Fig. 3). No significant hydrogen bonding or anion–π contacts are observed between the tetrafluoroborate anions and the host.

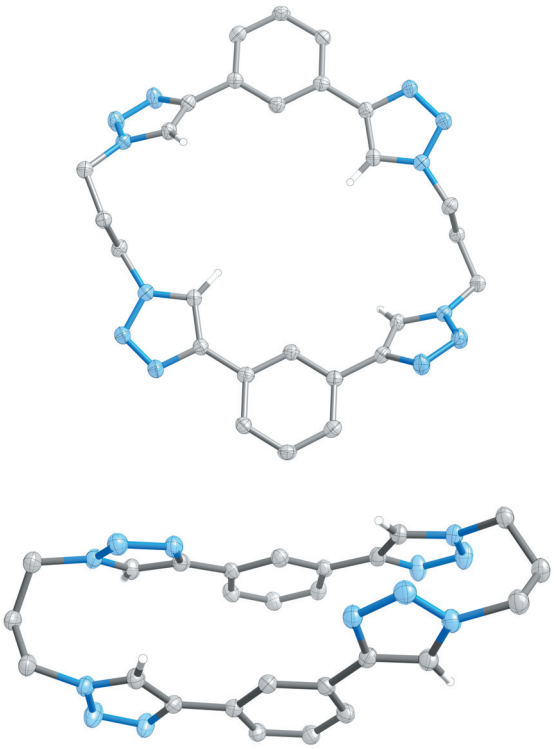

Fig. 2 Solid state structures of **2** when grown from DMSO–CH_2Cl_2 (top) and methanol–water (bottom). Ellipsoids shown at 50% probability; solvent molecules and some hydrogen atoms are omitted for clarity.

Anion binding studies

Neutral tetra-triazole macrocycles

Receptors **2** and **3** are insoluble in common organic solvents, but have sufficient solubility in d_6-DMSO to allow investigation of their anion binding properties *via* ^{1}H NMR titration experiments. Addition of aliquots of TBA·Cl to a solution of either **2** or **3** caused perturbation in the triazole signals, as well as smaller shifts in the phenylene and/or pyridyl protons. Job Plot analysis indicated 1 : 1 stoichiometric binding in solution. WINEQNMR2[42] analysis of the titration data, monitoring the triazole proton enabled association constants to be determined. As shown in Table 1, both macrocycles, **2** and **3** bind chloride weakly in this competitive solvent with the bis-phenylene receptor, **2**, displaying relatively stronger halide association than the pyridyl-substituted host, **3**. Association of cyclic tetra-alkyl receptor **1** and chloride was negligible in d_6-DMSO, and in less competitive 1 : 1 $CDCl_3$–CD_3CN. Even in CD_2Cl_2, the affinity of **1** for a range of anions (Cl^-, I^-, $C_6H_5CO_2^-$, SO_4^{2-}) was extremely weak ($K_a < 60$ M^{-1}).[43]

Tetra-triazolium macrocycle

Unfortunately, **7·BF$_4$** is insoluble in the 9 : 1 CD_3CN–D_2O solvent mixture used in our previous studies of tetra-imidazolium macrocycles.[33] Fluoride and chloride binding studies were instead conducted in 9 : 1 d_6-DMSO–D_2O, monitoring the four equivalent triazolium protons. Analysis of the titration data using

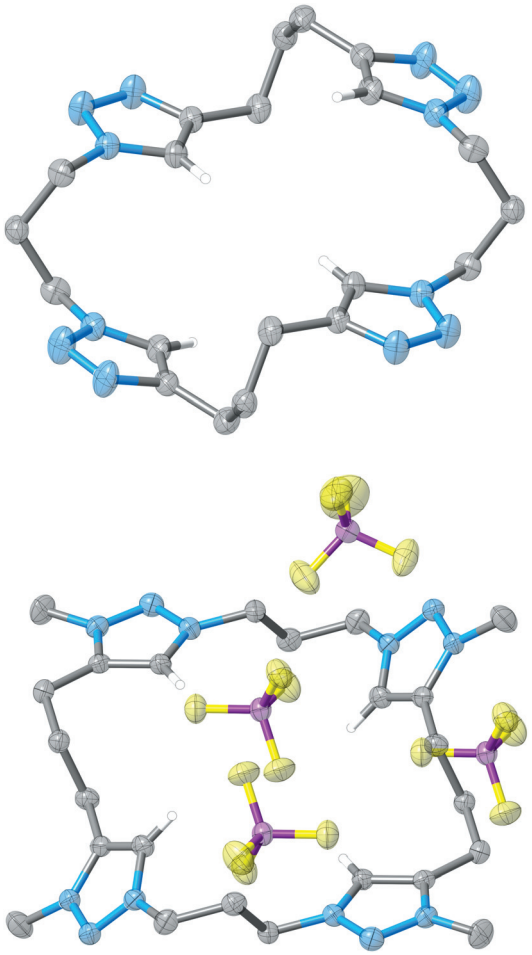

Fig. 3 Solid state structures of **1** (top) and **7·BF$_4$** (bottom). Ellipsoids shown at 50% probability; some hydrogen atoms are omitted for clarity.

Table 1 Association constants, K_a (M^{-1}) for tetra-triazole macrocycles with chloride anion; [a] estimated standard errors are given in parentheses

Solvent	1	2	3
d_6–DMSO	<10	77 (5)	37 (3)
1 : 1 $CDCl_3$–CD_3CN	<10	—	—
CD_2Cl_2	31 (3)	—	—

[a] Chloride added as tetrabutylammonium salt. Association constants calculated at 293 K, using WINEQNMR2.[42]

WINEQNMR2[42] showed very strong 1 : 1 stoichiometric binding of both halides ($K_a > 10^4$ M^{-1}), and so further titration experiments were undertaken in the more competitive 1 : 1 d_6-DMSO–D_2O aqueous mixture. As shown in Table 2 and Fig. 4, the macrocycle displays a preference for the larger halides, bromide and iodide, with all halides associating more strongly than the acetate oxoanion. The sulfate dianion is bound extremely strongly, presumably due to its doubly negative charge.

Interestingly, the anion binding trend displayed by **7·BF$_4$** (sulfate ≫ iodide > bromide > other monobasic anions) is similar to the trends reported by Kubik *et al.* for their neutral cyclic pseudo-peptide systems in methanol–water

Table 2 Association constants, K_a (M^{-1}) for **7·BF$_4$** and various anions; [a] estimated standard errors are given in parentheses

Anion	9 : 1 d_6-DMSO–D_2O	1 : 1 d_6-DMSO–D_2O
F^-	$>10^4$	226 (28)
Cl^-	$>10^4$	228 (5)
Br^-	—	388 (29)
I^-	—	463 (24)
OAc^-	—	148 (30)
SO_4^{2-}	—	$>10^4$

[a] Anions added as tetrabutylammonium salts. Association constants calculated at 293 K, using WINEQNMR2.[42]

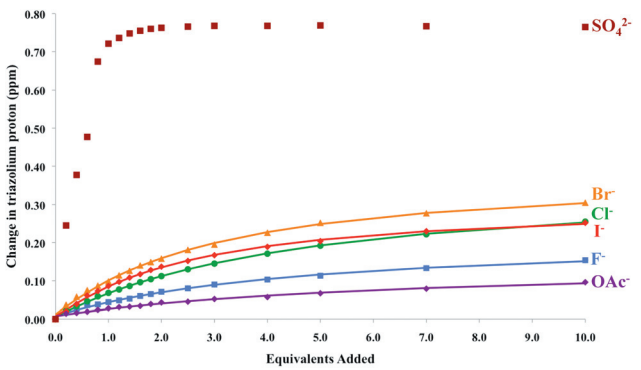

Fig. 4 Experimental titration data (solid points) and fitted binding isotherms (lines) for addition of TBA·anion to 1 : 1 d_6-DMSO–D_2O solutions of **7·BF$_4$**. Sulfate binding was too strong to allow determination of a binding constant using WINEQNMR2[42] ($K_a > 10^4$ M^{-1}).

mixtures,[22,23,25] where the observed selectivity is attributed to complementary host/guest size.

It is noteworthy that amongst the halides, the selectivity trend of **7·BF$_4$** is different from that of tetra-imidazolium and tetra-benzimidazolium analogues.[33] These receptors exhibit a pronounced selectivity for fluoride in 9 : 1 CD_3CN–D_2O, with other anions being bound only weakly, whereas **7·BF$_4$** preferentially binds bromide and iodide.[44]

Molecular modelling

The binding affinity of **7** for halide and sulfate anions in the competitive 1 : 1 DMSO–H_2O solvent mixture was also investigated by classical molecular dynamics (MD) simulations followed by quantum mechanics/molecular mechanics (QM/MM) simulations. These theoretical studies were performed with the AMBER 11 software package[45] as described in the ESI.† The starting binding arrangements of the sulfate and halide complexes were obtained in the gas phase by quenched MD simulations with **7** and the polyatomic anion described with the general amber force field (GAFF) parameters[46] and restrained electrostatic potential (RESP) atomic charges.[47] The monoatomic anions, with atomic charge set to −1, were described with van der Waals force field parameters developed for the transferable intermolecular potential three point (TIP3P) water model (See ESI†).[48]

The structures of the halide (F^-, Cl^-, Br^-, and I^-) and SO_4^{2-} complexes determined from gas phase MD simulations (see ESI†) were immersed in cubic boxes of a DMSO–H_2O (1 : 1) solvent mixture composed of 458 all atom DMSO molecules[49] and 1800 TIP3P water molecules.[50] The number of these molecules were calculated considering an equal volume of water and DMSO with densities of 1.00 and 1.10 g cm^{-3}, respectively. Furthermore, this total number of molecules led to equilibrated cubic boxes with side lengths (~47.7 Å), large enough to simulate the solvated complexes using a 10 Å cut-off for long-range electrostatic interactions and non-bonded van der Waals interactions. The complexes in these solvent boxes were subjected to classical MD simulation runs at room temperature (300 K) under periodic conditions following the multistage protocol described in the ESI.† However, all five anions were quickly solvated by the water molecules leaving irreversibly the macrocyle during the first 100 ps of the equilibration runs. In other words, these results show that the interaction of **7** with different anions is not appropriately described in this competitive solvent mixture using only electrostatic and van der Waals force field parameters. Hence, in an effort to understand the experimental binding data of **7** summarised in Table 2, we decided to investigate the anion complexes in the aqueous solvent mixture by QM/MM simulations using the same starting configurations, but with **7** and the anions described at the PM3 theory level and solvent molecules with classical force field parameters. The dynamical behaviours of the halide and sulfate anion complexes were evaluated for 2 ns using the previously equilibrated structures. Two extra replicates were carried out for fluoride and iodide complexes and equivalent sequences of events were observed as reported below. Representative snapshots taken from the QM/MM simulations of chloride, bromide and iodide complexes showing the anions surrounded by solvent molecules are presented in Fig. 5.

In these complexes the macrocycle almost preserves the flattened conformation (see ESI†), establishing with the anion (A) four intermittent C–H···A^- hydrogen bonds with average distances and standard deviations described in Table 3. The

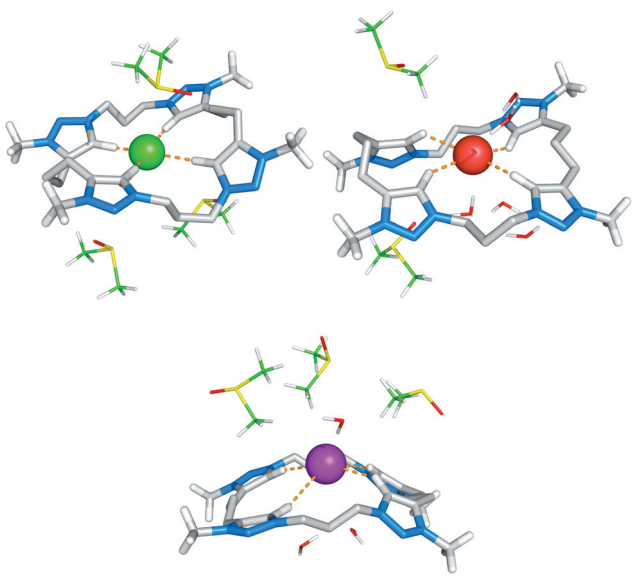

Fig. 5 Illustrative snapshots (QM/MD) of **7·Cl** (top, left), **7·Br** (top, right) and **7·I** (bottom) complexes showing the secondary anion solvent shell.

larger standard deviations estimated for H···I$^-$ distances indicate the charged assisted hydrogen bonding interactions were more often interrupted in the iodide complex than in the chloride and bromide complexes. They also reflect the prominent exposition of the largest halide anion to the water solvent molecules derived from the positions occupied by the anion, recurrently outside of the macrocyclic cavity, throughout the course of the QM/MM simulation. This structural feature will be further discussed below. In contrast, the smaller standard deviations for H···Br$^-$ distances suggest that among these three monoatomic anions, bromide is the more tightly bonded to **7**. Therefore, the understanding of the experimental binding preference of macrocycle for iodide requires the evaluation of other structural parameters as demonstrated below.

Conformational changes in the macrocycle **7** were also ascertained by measuring the distances between opposite triazolium C–H protons (H$_t$···H$_t$) on the macrocyclic backbone during the course of the QM/MM simulations. The corresponding average values are listed in Table 4 together with the distances of the anions to the mass centre of the macrocycle (A···C$_M$) defined here by all non-hydrogen atoms excluding the methyl substituents on the triazolium motifs.

In contrast with the chloride, bromide and iodide complexes, in which small variations in both H$_t$···H$_t$ distances were monitored, the fluoride complex has a drastic change in one of these distances as shown in Fig. 6 where they are plotted together with the four C–H···F$^-$ distances. During the first 898 ps of QM/MM simulation, the macrocycle exhibits an almost flattened conformation forming three uninterrupted hydrogen bonds with fluoride with identical average distances of 1.71, 1.69 and 1.71 Å (Table 3 first row). Subsequently, the complex undergoes a significant conformational change with **7** wrapping the fluoride anion in a folded fashion until the end of the simulation. This binding event is accompanied by a decrease of one H$_t$···H$_t$ distance (Table 4) and concomitant increase of the number of C–H···F$^-$ hydrogen bonding interactions from three to four. These structural findings show that the cavity provided by the flattened macrocyclic conformation is too large to accommodate the fluoride anion. Accordingly, **7** undertakes a conformational change with a substantial decrease of the macrocyclic cavity size in order to bind the smallest halide anion efficiently in a binding arrangement composed of four H···F$^-$ distances with small standard deviations (see Table 3). This conformational rearrangement is illustrated in Fig. 7 with three sequential snapshots taken from the QM/MM simulation.

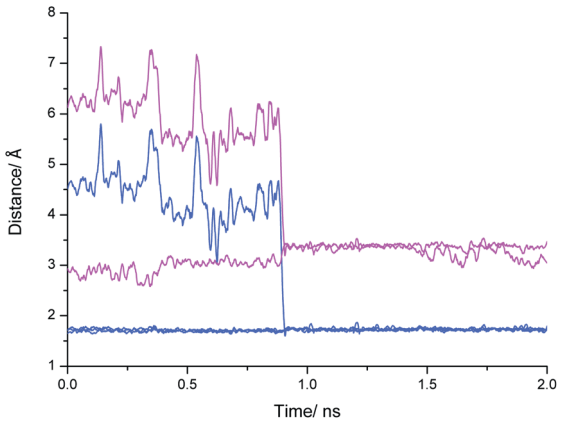

Fig. 6 Evolution of C–H···F$^-$ hydrogen bond (blue) distances and H$_t$···H$_t$ (magenta) distances along the QM/MM simulation of the fluoride complex.

Table 3 Average H···A distances (Å) with their standard deviations[a] between the anions and the four C–H triazolium groups

	H$_1$···A	**H$_2$···A**	**H$_3$···A**	**H$_4$···A**
F^{-b}	1.71 ± 0.08	1.69 ± 0.06	4.40 ± 0.58[d]	1.71 ± 0.07
	1.73 ± 0.07	*1.72 ± 0.06*	*1.73 ± 0.08*	*1.73 ± 0.07*
Cl$^-$	2.22 ± 0.52	2.17 ± 0.38	2.28 ± 0.48	2.36 ± 0.55
Br$^-$	2.64 ± 0.27	2.68 ± 0.31	2.64 ± 0.28	2.63 ± 0.25
I$^-$	3.31 ± 0.75	3.31 ± 0.79	3.12 ± 0.53	3.18 ± 0.76
SO_4^{2-}, O$_1$[c]	3.40 ± 0.75	3.71 ± 1.16	3.32 ± 0.84	2.94 ± 0.97
SO_4^{2-}, O$_2$[c]	3.13 ± 1.00	2.97 ± 1.18	3.20 ± 1.01	3.74 ± 0.47
SO_4^{2-}, O$_3$[c]	3.46 ± 0.95	3.90 ± 0.96	3.69 ± 0.68	3.36 ± 0.99
SO_4^{2-}, O$_4$[c]	3.15 ± 0.97	3.21 ± 1.04	3.00 ± 1.00	3.11 ± 0.98

[a] The standard deviations were calculated for N = 2000 with the exception of the values quoted for **7**·**F**, which were calculated with N = 898 for the first 898 ps of simulation and N = 1102 for the remaining simulation length. [b] The values in italics are for the folded binding arrangement. [c] The H···O distances listed for sulfate were calculated between each C–H triazolium group and the four oxygen atoms. [d] The large standard deviation for this measurement indicates that H$_3$ is not involved in hydrogen bonding interactions.

Table 4 Average H$_t$···H$_t$ and A···C$_M$ distances (Å) with their standard deviations[a]

	H$_1$···H$_3$	**H$_2$···H$_4$**	**A···C$_M$**
7	6.18 ± 0.78	6.59 ± 0.86	—
F^{-b}	5.96 ± 0.63	2.96 ± 0.20	1.29 ± 0.25
	3.30 ± 0.19	*3.37 ± 0.11*	*0.39 ± 0.25*
I$^-$	5.84 ± 0.65	5.88 ± 0.73	1.66 ± 0.72
SO_4^{2-}	5.29 ± 0.34	5.35 ± 0.62	2.27 ± 0.29

[a] The standard deviations were calculated for N = 2000 with the exception of the values quoted for **7**·**F**, which were calculated with N = 898 for the first 898 ps of simulation and N = 1102 for the remaining simulation length. [b] The values in italics are for the folded binding arrangement.

Further understanding of the binding selectivity of **7** for halide anions can be acquired by the comparison of the H$_t$···H$_t$ distances for the tetra-triazolium macrocycle in complexes and in free form. Hence, the free macrocycle was also submitted to a QM/MM run using the same simulation protocol. The H$_t$···H$_t$ average values listed in Table 4 for the free macrocycle are far from those reported for chloride and fluoride complexes. This is particularly evident for the latter complex, in which the macrocycle adopts a folded conformation to accommodate the smallest anion. In contrast, in the iodide complex, H$_t$···H$_t$ distances are much closer to the distances reported for the free macrocycle. This comparison suggests that the energetic cost associated with the conformational change of the macrocycle to bind the iodide is less than for the other halides, leading to a more stable complex.

The binding arrangement determined in the gas phase for the SO_4^{2-} complex (see ESI†) was not maintained in solution as can be seen from the snapshot taken at the beginning of the data collection run presented in Fig. 8. In fact, during the equilibration stage, the SO_4^{2-} left the macrocyclic cavity to form, with the

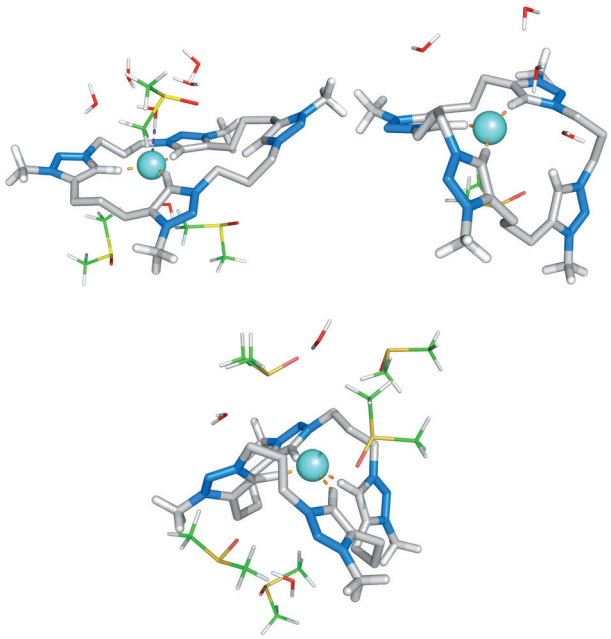

Fig. 7 Three representative snapshots of fluoride complex taken at the simulation times 0.160 (top-left), 0.899 (top-right) and 2 (bottom) ns showing the different binding arrangements observed throughout the course of the QM/MM simulation length.

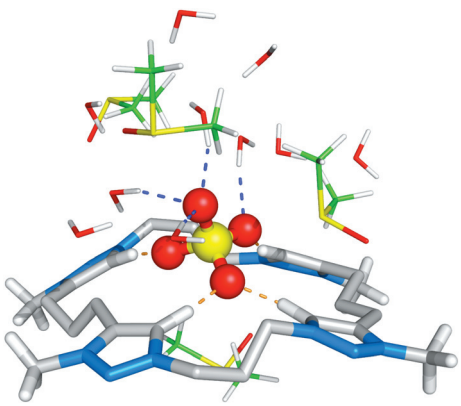

Fig. 8 Snapshot of **7·SO$_4$** complex taken at the beginning of the production run illustrating the binding pose adopted by the sulphate anion along the QM/MM simulation. The anion is exposed to the solvent molecules establishing O–H···O hydrogen bonds with several waters, drawn as blue dashed lines.

four C–H triazolium protons, multiple C–H···O hydrogen bonding interactions based on the intermittent swapping of all oxygen atoms, as evident by the large standard deviations determined for H···O distances measured along the simulation length (see Table 3).

The average A···C$_M$ distances listed in Table 4 for **7·Cl**, **7·Br** and **7·I** complexes reflect the anion size order ($I^- > Br^- > Cl^-$) being determined by the fitting between the size of each anion and the cavity size of the flattened macrocyclic conformation. Thus, the larger anions I^- (1.66 Å) and SO_4^{2-} (2.27 Å) are clearly positioned outside of the macrocycle whereas the smaller anions Br^- (0.55 Å) and Cl^- (0.49 Å) are barely out of **7**.

Table 5 Average number of solvent molecules enclosing the anions within the 1st and 2nd shells with *radii* of 3.4 and 5.0 Å respectively[a]

	DMSO		H_2O	
	1st	2nd	1st	2nd
F^-	0.6 (0–3)	2.1	0.5 (0–3)	3.6
Cl^-	0.8 (0–3)	2.1	0.7 (0–3)	3.8
Br^-	0.7 (0–3)	2.5	1.7 (0–4)	4.7
I^-	0.7 (0–3)	3.0	1.5 (0–5)	3.8
SO_4^{2-}	0.5 (0–3)	1.6	5.9 (2–10)	9.3

[a] The maximum and minimum number found in both coordination spheres are given in parentheses.

However, the smaller standard deviations obtained for C–H···Br^- hydrogen interactions indicate that the strength of the interaction between Br^- and the macrocycle is stronger than with Cl^-, which is agreement with experimental binding data for these two anions. The average F^-···C$_M$ distance during the first 898 ps where the macrocycle also adopts a flattened conformation is 1.29 Å in agreement with existence of three C–H···F^- interactions only.

Solvent effects

The impact of the competitive 1 : 1 DMSO–H_2O solvent mixture on the binding affinity of **7** for halides and sulfate anions was ascertained by calculating the number of water and DMSO molecules around each anion along the QM/MM simulations (see Table 5).

It is clear that in **7·Br**, **7·I**, and **7·SO$_4$** complexes, the anion is preferentially solvated by water molecules in the first solvation shell while in **7·F** and **7·Cl** complexes, the anion is surrounded by an equivalent smaller number of water and DMSO solvent molecules. This fact is understandable considering that the two smaller anions are sheltered from both solvent molecules by the macrocycle. Indeed, the chloride anion is barely outside of the flattened macrocyclic conformation while the fluoride anion is wrapped by the folded macrocyclic conformation during most of the simulation time. In contrast, I^- and SO_4^{2-} anions, as shown above, are positioned outside of the macrocycle exposed to the competitive water molecules, in particular the polyatomic anion. Nonetheless, the average number of water molecules within the first solvation shell of bromide (1.7) is slightly higher than in the iodide (1.5) not reflecting the Br···C$_M$ and I···C$_M$ distances, as would be expected. This surprising result corroborates the experimental binding data of **7·Br** and **7·I** complexes (see Table 2), when they are compared alone.

As expected, in all complexes the extent of anion solvation increases in the second coordination sphere, which is preferentially composed of water molecules. This is consistent with the cubic box used to simulate the 1 : 1 DMSO–H_2O competitive solvent mixture, which contained predominantly water molecules, and with the cut-off used to compute the number of both solvent molecules in the second shell of 5.0 Å, which is proximal to the bulk solvent. The significant number of DMSO molecules surrounding the anions, in particular in the case of halide complexes, reflects the solvation of the tetra-triazolium

macrocycle by a large number of DMSO molecules. This is particularly evident for the iodide complex with an average of three DMSO molecules protecting the iodide from extensive solvation by coordinating water molecules.

The sulfate anion is widely solvated by water molecules in both solvation shells and consequently, the experimental binding preference of **7** for the sulfate anion seems to be dictated by the net charges of both partners, in other words, by the strength of the electrostatic interactions between charged tetra-imidazolium macrocycle (+4) and SO_4^{2-}.

In conclusion the modelling studies show that the affinity of **7** for the different anions is governed by multiple charged assisted C–H···A^- interactions in which the steric requirements imposed by the apparently rigid macrocyclic backbone together with solvation effects seem to have an important role.

Conclusions

We have prepared three tetra-triazole macrocycles in good yield using a CuAAC cyclisation of triazole bis-azides and bis-alkynes. One of these macrocycles was successfully alkylated to give the tetra-triazolium host, **7**·$\mathbf{BF_4}$. This receptor binds anions strongly by charge-assisted C–H···anion hydrogen bonding, even in the competitive 1 : 1 d_6-DMSO–D_2O aqueous solvent mixture. Among the halides, iodide and bromide associate more strongly than chloride and fluoride, and all halides form stronger complexes than acetate. The sulfate dianion is bound extremely strongly, with an association constant greater than 10^4 M^{-1}. The observed solution anion binding trends are supported by extensive molecular modelling analysis, which suggest macrocycle cavity size, solvation effects and strength of electrostatic interactions significantly influence the observed anion recognition processes. Hence, this paper demonstrates that the incorporation of multiple triazolium motifs into a cyclic host framework produces a potent anion receptor that functions in aqueous solvent mixtures.

Experimental

General remarks

CAUTION: Low molecular weight organic azides are potentially explosive. While no problems were encountered in the course of this work, they should be handled in small quantities and with appropriate care.

TBTA[51] and 3-azidopropoxytosylate, **4**,[41] were prepared as previously described. 3,5-Diethynylpyridine was prepared by deprotecting 3,5-bis(trimethylsilylethynyl)-pyridine[52] using KOH in methanol.[53] Other chemicals were available commercially and used as received. Where solvents are specified as "dry", they were purged with nitrogen and passed through an MBraun MPSP-800 column. Water was de-ionised and microfiltered using a Milli-Q Millipore machine. Tetrabutylammonium salts were stored in a vacuum dessicator. All chromatography was performed on silica gel (particle size: 40–63 μm).

Routine NMR spectra were recorded on a Varian Mercury 300 spectrometer with 1H NMR operating at 300 MHz, 13 °C at 75.5 MHz. Spectra for 1H NMR titrations were recorded on a Varian Unity Plus 500 spectrometer with 1H operating at 500 MHz. Mass spectra were recorded on a Bruker microTOF spectrometer. Copies of NMR spectra and titration protocols are detailed in the ESI.†

Phenyl bis-triazolyl azide, 5. 1,3-Diethylnyl benzene (0.359 mL, 0.341 g, 2.70 mmol) and tosyl-protected azide, **4**, (1.45 g, 5.67 mmol, 2.1 equiv) were dissolved in dry dichloromethane (60 mL). DIPEA (1.1 mL, 0.78 g, 6.0 mmol), TBTA (0.287 g, 0.540 mmol) and $[Cu^I(CH^3CN)^4(PF^6)$ (0.202 g, 0.540 mmol) were added and the resulting pale yellow solution stirred at room temperature under a nitrogen atmosphere for 4 days. It was taken to dryness under reduced pressure and purified by column chromatography (3% methanol in dichloromethane) to give a pale yellow foam, which was used immediately to prepare **5**.

^{1}H NMR ($CDCl_3$): 8.20 (s, 2H, 2 × trz-*H*), 7.75–7.83 (m, 7H, 4 × Ts-*H*, 3 × Ph-*H*), 7.50 (t, ^3J = 7.7 Hz, 1H, Ph-*H*), 7.33 (d, ^3J = 8.0 Hz, 4H, 4 × Ts-*H*), 4.51 (t, ^3J = 6.6 Hz, 4H, 4 × CH_2-trz), 4.06 (t, ^3J = 5.7 Hz, 4H, 4 × TsO-CH_2), 2.31–2.43 (m, 10H, 6 × CH_3, 4 × CH_2-CH_2-CH_2). LRESI-MS (pos.): 659.26, calc. for $[C_{30}H_{32}N_6O_6S_2{\cdot}Na]^+$ = 659.17.

The ditosylate, was dissolved in DMSO (25 mL). Sodium azide (0.478 g, 7.35 mmol, 2.50 equiv) was added and the mixture heated at 60 °C under a nitrogen atmosphere over the weekend. It was cooled to room temperature, and partitioned between water and (100 mL each). The organic layer was taken and the aqueous layer extracted further with (100 mL). The combined organic fractions were washed with water (100 mL), saturated brine (100 mL) and dried (magnesium sulfate), taken to dryness under reduced pressure and purified by column chromatography (2% methanol in dichloromethane) to give **5** as a pale yellow foamy solid. Yield: 0.773 g (76% from 1,3-diethynylbenzene).

^{1}H NMR ($CDCl_3$): 8.29 (s, 2H, 2 × 2 × trz-*H*), 7.82–7.87 (m, 3H, 3 × Ph-*H*), 7.51 (t, ^3J = 7.7 Hz, 1H, Ph-*H*), 4.53 (t, ^3J = 6.7 Hz, 4H, 4 × CH_2-trz), 3.41 (t, ^3J = 6.3 Hz, 4H, 4 × CH_2-N_3), 2.17–2.31 (m, 4H, CH_2-CH_2-CH_2). ^{13}C NMR ($CDCl_3$): 147.3, 131.1, 129.5, 125.3, 122.8, 120.4, 48.0, 47.3, 29.4. LRESI-MS (pos.): 401.18, calc. for $[C_{16}H_{18}N_{12}{\cdot}Na]^+$ = 401.17; 779.38, calc. for $[C_{32}H_{36}N_{24}{\cdot}Na]^+$, *i.e.* $[M_2{\cdot}Na]^+$ = 779.35. HRESI-MS (pos.): 401.1667, calc for $[C_{16}H_{18}N_{12}{\cdot}Na]^+$ = 401.1670.

Propyl bis-triazolyl azide, 6. 1,6-Heptadiyne (0.103 mL, 0.083 g, 0.90 mmol) and tosyl-protected azide, **4**, (0.482 g, 1.89 mmol, 2.1 equiv.) were dissolved in dichloromethane (25 mL). DIPEA (0.35 mL, 0.26 g, 2.00 mmol), TBTA (0.096 g, 0.18 mmol) and $[Cu^I(CH_3CN)_4(PF_6)$ (0.067 g, 0.18 mmol) were added and the resulting pale yellow solution stirred at room temperature under a nitrogen atmosphere overnight. It was taken to dryness under reduced pressure and purified by column chromatography (2% methanol in chloroform) to give a yellow oil. This was used immediately to prepare **6**.

^{1}H NMR ($CDCl_3$): 7.75–7.79 (m, 4H, 4 × Ts-*H*), 7.33–7.37 (m, 4H, 4 × Ts-*H*), 7.29 (s, 2H, 2 × trz-*H*), 4.40 (t, ^3J = 6.7 Hz, 4H, 4 × trzN-CH_2), 4.00 (t, ^3J = 5.7 Hz, 4H, 4 × TsO-CH_2), 2.73 (t, ^3J = 7.5 Hz, 4H, 4 × trzC-CH_2), 2.44 (s, 6H, 6 × CH_3), 2.23–2.32 (m, 4H, 4 × TsO-CH_2-CH_2), 1.97–2.07 (m, 2H, 2 × trzC-CH_2-CH_2). LRESI-MS (pos.): 625.23, calc. for $[C_{27}H_{34}N_6O_6S_2{\cdot}Na]^+$ = 625.19.

The ditosylate, was dissolved in dimethylsulfoxide (10 mL). Sodium azide (0.234 g, 3.60 mmol) was added and the mixture heated at 60 °C under a nitrogen atmosphere over the weekend. It was cooled to room temperature, and partitioned between water and diethyl ether (100 mL each). The organic layer was taken and the aqueous layer extracted further with diethyl ether (100 mL). The combined organic fractions were dried (magnesium sulfate), taken to dryness under reduced pressure and purified by column chromatography (1.5% methanol in dichloromethane) to give **6** as a pale yellow oil. Yield: 0.093 g (30% from 1,6-heptadiyne).

^{1}H NMR ($CDCl_3$): 7.37 (s, 2H, 2 × trz-*H*), 4.47 (t, ^3J = 6.6 Hz, 4H, 4 × trzN-CH_2), 3.41 (t, ^3J = 6.4 Hz, 4H, 4 × CH_2-N_3), 2.73 (t, ^3J = 8.8 Hz, 4H, 4 × trzC-CH_2), 1.95–2.25 (m, 6H, 4 × N_3-CH_2-CH_2, 2 × trzC-CH_2-CH_2). ^{13}C NMR ($CDCl_3$): 147.8, 121.5, 48.2, 47.1, 29.6, 29.2, 25.0. LRESI-MS (pos.): 367.19, calc. for $[C_{13}H_{20}N_{12}{\cdot}Na]^+$ = 367.18; 711.40, calc. for $[C_{26}H_{40}N_{24}{\cdot}Na]^+$, *i.e.* $[M_2{\cdot}Na]^+$ = 711.38. HRESI-MS (pos.): 367.1826, calc. for $[C_{13}H_{20}N_{12}{\cdot}Na]^+$ = 367.1826.

Phenyl-linked tetra-triazole macrocycle, 2. The bis-azide, **5**, (0.151 g, 0.400 mmol) and 1,3-diethynylbenzene (0.0532 mL, 0.0505 g, 0.400 mmol) were dissolved in dichloromethane (400 mL). DIPEA (0.17 mL, 0.13 g, 1.0 mmol), TBTA (0.042 g, 0.080 mmol) and $[Cu^I(CH_3CN)_4](PF_6)$ (0.030 g, 0.080 mmol) were added and the pale yellow solution stirred for 4 days under a nitrogen atmosphere, during which time a fluffy yellow precipitate developed. The reaction mixture was taken to dryness under reduced pressure and purified by column chromatography (gradient: 5–10% methanol in dichloromethane) to give **2** as a white powder. Yield: 0.136 g (67%).

^{1}H NMR (d_6-DMSO): 8.11 (s, 4H, 4 × trz-*H*), 7.98 (t, ^4J = 1.4 Hz, 2H, 2 × Ph-*H*), 7.56 (dd, ^3J = 7.5 Hz, ^4J = 1.4 Hz, 4H, 4 × Ph-*H*), 7.30 (t, ^3J = 7.5 Hz, 2H, 2 × Ph-*H*), 4.53 (t, ^3J = 5.3 Hz, 8H, 8 × trz-CH_2), 2.68 (qn, ^3J = 5.3 Hz, 4H, 4 × CH_2-CH_2). ^{13}C NMR (d_6-DMSO): 146.1, 130.8, 128.9, 123.9, 122.4, 121.3, 47.9, 29.2. LRESI-MS (neg.): 539.18, calc. for $[C_{26}H_{24}N_{12}{\cdot}Cl]^-$ = 539.19. HRESI-MS (neg.): 539.1936, calc. for $[C_{26}H_{24}N_{12}{\cdot}Cl]^-$ = 539.1941.

Pyridyl-linked tetra-triazole macrocycle, 3. The bis-azide, **5**, (0.265 g, 0.700 mmol) and 3,5-diethynylpyridine (0.0890 g, 0.700 mmol) were dissolved in dichloromethane (700 mL). DIPEA (0.31 mL, 0.24 g, 1.0 mmol), TBTA (0.074 g, 0.14 mmol) and $[Cu^I(CH_3CN)_4](PF_6)$ (0.052 g, 0.14 mmol) were added and the pale yellow solution stirred for three days under a nitrogen atmosphere at room temperature, during which time a pale precipitate developed. It was taken to dryness under reduced pressure and purified by column chromatography (gradient: 10–15% dichloromethane in methanol) to give **3** as a white powder. Yield: 0.208 g (59%).

^{1}H NMR (d_6-DMSO): 8.56 (br. s, 2H, 2 × py-$H_{2,6}$), 8.10 (t, ^4J = 1.9 Hz, 1H, py-H_4), 8.05 (s, 2H, 2 × trz-*H*), 7.91 (s, 2H, 2 × trz-*H*), 7.84 (t, ^4J = 1.5 Hz, 1H, Ph-*H*), 7.36 (dd, ^3J = 7.7 Hz, ^4J = 1.5 Hz, 2H, 2 × Ph-*H*), 7.20 (t, ^3J = 7.7 Hz, 2 × Ph-H), 4.58–4.64 (m, 8H, 8 × trz-CH_2, 4 × H_g), 2.66–2.76 (m, 4H, 4 × trz-CH_2-CH_2). ^{13}C NMR (d_6-DMSO): 146.0, 144.8, 143.2, 130.6, 128.7, 128.3, 126.2, 124.0, 121.6, 121.3, 120.9, 48.8, 48.6, 28.8. LRESI-MS (pos.): 528.25, calc. for $[C_{25}H_{23}N_{13}{\cdot}Na]^+$ = 528.21; 1033.55, calc. for $[C_{50}H_{46}N_{26}{\cdot}Na]^+$, *i.e.* $[M_2{\cdot}Na]^+$ = 1033.43. LRESI-MS (neg.): 540.19, calc. for $[C_{25}H_{23}N_{13}{\cdot}Cl]^-$ = 540.19; 1045.42, calc. for $[C_{50}H_{46}N_{26}{\cdot}Cl]^-$, *i.e.* $[M_2{\cdot}Cl]^-$ = 1045.41. HRESI-MS (pos.): 528.2081, calc. for $[C_{25}H_{23}N_{13}{\cdot}Na]^+$ = 528.2092.

Propyl-linked tetra-triazole macrocycle, 1. The bis-azide, **6** (0.069 g, 0.20 mmol) and 1,6-heptadiyne (0.023 mL, 0.018 g, 0.20 mmol) were dissolved in dichloromethane (200 mL). DIPEA (0.035 mL, 0.026 g, 0.20 mmol), TBTA (0.021 g, 0.040 mmol) and $[Cu^I(CH_3CN)_4](PF_6)$ (0.015 g, 0.040 mmol) were added and the yellow solution stirred at room temperature under a nitrogen atmosphere for 3 days. It was concentrated to ~50 mL under reduced pressure and filtered, with the precipitate washed thoroughly with 10% methanol in dichloromethane. The combined filtrates were taken to dryness under reduced pressure and purified by column chromatography (gradient: 5–15% methanol in chloroform) to give **1** as a white powder. Yield: 0.043 g (49%).

^{1}H NMR ($CDCl_3$): 7.41 (s, 4H, 4 × trz-*H*), 4.29 (t, ^3J = 6.2 Hz, 8H, 8 × trzN-CH_2), 2.64–2.73 (m, 12H, 8 × trzC-CH_2, 4 × trzN-CH_2), 2.09 (qn, ^3J = 6.9 Hz, 4H, 4 × trzC-CH_2). ^{13}C NMR ($CDCl_3$): 147.3, 122.9, 46.5, 29.5, 28.3, 23.9. LRESI-MS (pos.): 459.28, calc. for $[C_{20}H_{28}N_{12}{\cdot}Na]^+$ = 459.25; 895.59, calc. for $[C_{40}H_{56}N_{24}{\cdot}Na]$, *i.e.* $[M_2{\cdot}Na]^+$ = 895.50. LRESI-MS (neg): 471.23, calc. for $[C_{20}H_{28}N_{12}{\cdot}Cl]^-$ = 471.23. HRESI-MS (pos.): 459.2455, calc. for $[C_{20}H_{28}N_{12}{\cdot}Na]^+$ = 459.2452.

Propyl-linked tetra-triazolium macrocycle, 7 $(BF_4)_4$. The neutral macrocycle, **1** (0.022 g, 0.050 mmol) was dissolved in dry dichloromethane (20 mL). Trimethyloxonium tetrafluoroborate (0.037 g, 0.25 mmol) was added and the mixture stirred at room temperature under a nitrogen atmosphere for 2 days. Methanol (1 mL) was added and the solution taken to dryness under reduced pressure. The crude solid was stirred in dichloromethane (15 mL); the supernatant fluid was decanted and the resulting white powder washed with further dichloromethane (10 mL). The solid was recrystallised from boiling 6 : 1 ethanol–acetonitrile to give **7**·4$(BF_4)_4$ as large white needle crystals. Yield: 0.023 g (54%).

^{1}H NMR (d_6-DMSO): 8.47 (s, 4H, 4 × trz$^+$-*H*), 4.69 (t, ^3J = 7.0 Hz, 8H, 8 × trzN-CH_2), 4.22 (s, 12H, 12 × CH_3), 2.96 (t, ^3J = 7.0 Hz, 8H, 8 × trzC-CH_2), 2.48–2.54 (m, obscured by DMSO solvent peak, 4 × trzN-CH_2-CH_2), 2.02–2.08 (m, 4H, 4 × trzC-C_2-CH_2). ^{19}F NMR (d_6-DMSO): −148.4 (m). ^{13}C NMR (d_6-DMSO): 143.8, 128.0, 49.5, 37.5, 28.8, 23.8, 21.6. LRESI-MS (pos.): 335.18, calc. for $[(C_{24}H_{40}N_{12}){\cdot}2(BF_4)]^{2+}$ = 335.18; 757.38, calc. for $[(C_{24}H_{40}N_{12}){\cdot}3(BF_4)]^+$ = 757.36. HRESI-MS (pos.): 757.3593, calc. for $[(C_{24}H_{40}N_{12}){\cdot}3(BF_4)]^+$ = 757.3581.

X-ray crystallography

Single crystal X-ray diffraction data for **2** from DMSO–CH_2Cl_2 and from methanol–water were collected using graphite monochromated Mo Kα radiation (λ = 0.71073 Å) on a Nonius Kappa CCD diffractometer equipped with a Cryostream N2 open-flow cooling device,[54] and the data were collected at 150(2) K. Series of ω-scans were performed in such a way as to collect all unique

reflections to a maximum of 0.80 Å. Cell parameters and intensity data (including inter-frame scaling) were processed using the DENZO-SMN package.[55] Single crystal X-ray diffraction data for **1** and **7·BF$_4$** were collected using graphite monochromated Cu Kα radiation (λ = 1.54184 Å) on an Oxford Diffraction SuperNova diffractometer. The diffractometer was equipped with a Cryostream N2 open-flow cooling device,[54] and the data were collected at 150(2) K. Series of ω-scans were performed in such a way as to collect all unique reflections to a maximum of 0.80 Å. Cell parameters and intensity data (including inter-frame scaling) were processed using CrysAlis Pro.[56] The structures were solved by charge-flipping methods using SUPERFLIP[57] and refined using full-matrix least-squares on F^2 within the CRYSTALS suite.[58] All non-hydrogen atoms were refined with anisotropic displacement parameters. Hydrogen atoms were generally visible in the difference map and their positions and displacement parameters were refined using restraints prior to inclusion into the model using riding constraints.[59] Crystallographic data for the structures have been deposited with the Cambridge Crystallographic Data Centre, CCDC: 881646–881649.†

Acknowledgements

We thank Oxford Chemical Crystallography for the use of instruments, and Dr Amber L. Thompson for helpful discussions. NGW thanks the Clarendon Fund and Trinity College, Oxford for funding. SC thanks the FCT for the post-doctoral fellowship SFRH /BPD/42357/2007.

References

1 V. Rostovtsev, L. Green, V. Fokin and K. Sharpless, *Angew. Chem., Int. Ed.*, 2002, **41**, 2596–2599.
2 C. Tornoe, C. Christensen and M. Meldal, *J. Org. Chem.*, 2002, **67**, 3057–3064.
3 Y. Li and A. H. Flood, *Angew. Chem., Int. Ed.*, 2008, **47**, 2649–2652.
4 Y. Li and A. H. Flood, *J. Am. Chem. Soc.*, 2008, **130**, 12111–12222.
5 H. Juwarker, J. M. Lenhardt, D. M. Pham and S. L. Craig, *Angew. Chem., Int. Ed.*, 2008, **47**, 3740–3743.
6 R. M. Meudtner and S. Hecht, *Angew. Chem., Int. Ed.*, 2008, **47**, 4926–4930.
7 H. Juwarker, J. M. Lenhardt, J. C. Castillo, E. Zhao, S. Krishnamurthy, R. M. Jamiolkowski, K. H. Kim and S. L. Craig, *J. Org. Chem.*, 2009, **74**, 8924–8934.
8 Y. Wang, F. Bie and H. Jiang, *Org. Lett.*, 2010, **12**, 3630–3633.
9 S. Lee, Y. Hua and A. Flood, *Org. Lett.*, 2010, **12**, 2100–2102.
10 Y. Hua and A. Flood, *J. Am. Chem. Soc.*, 2010, **132**, 12838–12840.
11 Q.-Y. Cao, T. Pradhan, S. Kim and J. Kim, *Org. Lett.*, 2011, **13**, 4386–4389.
12 Y. Wang, J. Xiang and H. Jiang, *Chem.–Eur. J.*, 2011, **17**, 613–619.
13 K. McDonald, R. Ramabhadran, S. Lee, K. Raghavachari and A. Flood, *Org. Lett.*, 2011, **13**, 6260–6263.
14 Y. Li, M. Pink, J. A. Karty and A. H. Flood, *J. Am. Chem. Soc.*, 2008, **130**, 17293–17295.
15 R. O. Ramabhadran, Y. Hua, Y.-j. Li, A. H. Flood and K. Raghavachari, *Chem.–Eur. J.*, 2011, **17**, 9123–9129.
16 Y. Hua, R. O. Ramabhadran, E. O. Uduchi, J. A. Karty, K. Raghavachari and A. H. Flood, *Chem.–Eur. J.*, 2011, **17**, 312–321.
17 V. Haridas, S. Sahu and P. Venugopalan, *Tetrahedron*, 2011, **67**, 727–733.
18 M. R. Krause, R. Goddard and S. Kubik, *J. Org. Chem.*, 2011, **76**, 7084–7095.
19 Y. Lau, P. Rutledge, M. Watkinson and M. Todd, *Chem. Soc. Rev.*, 2011, **40**, 2848–2866.
20 C.-H. Lee, S. Lee, H. Yoon and W.-D. Jang, *Chem.–Eur. J.*, 2011, **17**, 13898–13903.
21 Y. Hua, R. Ramabhadran, J. Karty, K. Raghavachari and A. Flood, *Chem. Commun.*, 2011, **47**, 5979–5981.
22 S. Kubik, R. Goddard, R. Kirchner, D. Nolting and J. Seidel, *Angew. Chem., Int. Ed.*, 2001, **40**, 2648–2651.
23 S. Kubik and R. Goddard, *Proc. Natl. Acad. Sci. U. S. A.*, 2002, **99**, 5127–5132.
24 I. E. Drubi Vega, S. Camiolo, P. A. Gale, M. B. Hursthouse and M. E. Light, *Chem. Commun.*, 2003, 1686–1687.
25 S. Kubik, R. Kirchner, D. Nolting and J. Seidel, *J. Am. Chem. Soc.*, 2002, **124**, 12752–12760.
26 Z. Rodriguez-Docampo, S. Pascu, S. Kubik and S. Otto, *J. Am. Chem. Soc.*, 2006, **128**, 11206–11210.
27 R. Yang, W.-X. Liu, H. Shen, H.-H. Huang and Y.-B. Jiang, *J. Phys. Chem. B*, 2008, **112**, 5105–5110.
28 C. Caltagirone, J. R. Hiscock, M. B. Hursthouse, M. E. Light and P. A. Gale, *Chem.–Eur. J.*, 2008, **14**, 10236–10243.
29 R. Vilar, *Eur. J. Inorg. Chem.*, 2008, 357–367.
30 P. Ballester, *Chem. Soc. Rev.*, 2010, **39**, 3810–3830.
31 S. Kubik, *Chem. Soc. Rev.*, 2010, **39**, 3648–3663.
32 D. Mercer and S. Loeb, *Chem. Soc. Rev.*, 2010, **39**, 3612–3620.
33 W. W. H. Wong, M. S. Vickers, A. R. Cowley, R. L. Paul and P. D. Beer, *Org. Biomol. Chem.*, 2005, **3**, 4201–4208.
34 A. Kumar and P. S. Pandey, *Org. Lett.*, 2008, **10**, 165–168.
35 K. M. Mullen, J. Mercurio, C. J. Serpell and P. D. Beer, *Angew. Chem., Int. Ed.*, 2009, **48**, 4781.
36 B. Schulze, C. Friebe, M. Hager, W. Günther, U. Köhn, B. Jahn, H. Görls and U. Schubert, *Org. Lett.*, 2010, **12**, 2710–2713.
37 K. Ohmatsu, M. Kiyokawa and T. Ooi, *J. Am. Chem. Soc.*, 2011, **133**, 1307–1309.
38 R. Chhatra, A. Kumar and P. S. Pandey, *J. Org. Chem.*, 2011, **76**, 9086–9089.
39 L. C. Gilday, N. G. White and P. D. Beer, *Dalton Trans.*, 2012, **41**, 7092–7097.
40 N. G. White and P. D. Beer, *Beilstein J. Org. Chem.*, 2012, **8**, 246–252.
41 V. Aucagne, K. Hanni, D. Leigh, P. Lusby and D. Walker, *J. Am. Chem. Soc.*, 2006, **128**, 2186–2187.
42 M. J. Hynes, *J. Chem. Soc., Dalton Trans.*, 1993, 311–312.
43 Presumably this is at least partly due to the tight ion-pairing of TBA salts in chlorinated solvents. See ref. 16 and S. Alunni, A. Pero and G. Reichenbach, *J. Chem. Soc., Perkin Trans. 2*, 1998, 1747–1750.
44 Kim has recently reported a larger tetra-imidazolium receptor, which binds iodide in preference to the smaller halides or acetate in 9 : 1 CD_3CN–D_2O. V. Suresh, N. Ahmed, I. S. Youn and K. S. Kim, *Chem.–Asian J.*, 2012, **7**, 658–663.
45 D. A. Case, T. A. Darden, T. E. Cheatham, III, C. L. Simmerling, J. Wang, R. E. Duke, R. Luo, M. Crowley, R. C. Walker, W. Zhang, K. M. Merz, B. Wang, S. Hayik, A. Roitberg, G. Seabra, I. Kolossváry, K. F. Wong, F. Paesani, J. Vanicek, X. Wu, S. R. Brozell, T. Steinbrecher, H. Gohlke, L. Yang, C. Tan, J. Mongan, V. Hornak, G. Cui, D. H. Mathews, M. G. Seetin, C. Sagui, V. Babin and P. A. Kollman, *AMBER11*, 2010.
46 J. Wang, R. M. Wolf, J. W. Caldwell, P. A. Kollman and D. Case, *J. Comput. Chem.*, 2004, **25**, 1157–1174.
47 R. Bayly, P. Cieplak, W. Cornell and P. Kollman, *J. Phys. Chem.*, 1993, **97**, 10269–10280.
48 I. S. Young and T. E. Cheatham, III, *J. Phys. Chem. B*, 2008, **112**, 9020–9041.
49 T. Fox and P. A. Kollman, *J. Phys. Chem. B*, 1998, **102**, 8070–8079.
50 W. L. Jorgensen, J. Chandrasekhar, J. D. Madura, R. Impey and M. L. Klein, *J. Chem. Phys.*, 1983, **79**, 926–935.
51 B.-Y. Lee, S. R. Park, H. B. Jeon and K. S. Kim, *Tetrahedron Lett.*, 2006, **47**, 5105–5109.
52 H. Goto, J. Heemstra, D. Hill and J. Moore, *Org. Lett.*, 2004, **6**, 889–892.
53 T. X. Neenan and G. M. Whitesides, *J. Org. Chem.*, 1988, **53**, 2489–2496.
54 J. Cosier and A. M. Glazer, *J. Appl. Crystallogr.*, 1986, **19**, 105–107.
55 Z. Otwinowski and W. Minor, in *Methods Enzymol.*, ed. C. W. Carter and R. M. Sweet, Academic Press, 1997, ch. 276.
56 Agilent Technologies, *CrysAlisPro*, 2011.
57 L. Palatinus and G. Chapuis, *J. Appl. Crystallogr.*, 2007, **40**, 786–790.
58 P. W. Betteridge, J. R. Carruthers, R. I. Cooper, K. Prout and D. J. Watkin, *J. Appl. Crystallogr.*, 2003, **36**, 1487.
59 R. I. Cooper, A. L. Thompson and D. J. Watkin, *J. Appl. Crystallogr.*, 2010, **43**, 1017–1022.